

Dynamics of broadband accumulated spectral gratings in $\text{Tm}^{3+}:\text{YAG}$

Mingzhen Tian, Jun Zhao, Zachary Cole, Randy Reibel, and William Randall Babbitt

Department of Physics, Montana State University, Bozeman, Montana 59717-3840

High-bandwidth accumulated spectral gratings are experimentally studied in $\text{Tm}^{3+}:\text{YAG}$ by the stimulated-photon-echo technique with a mode-locked picosecond Ti:sapphire laser system. The experimental results show that the spectral grating builds up and decays on the time scale of the metastable-state lifetime (~ 10 ms), provided that the time interval of accumulating shots is of the order of the excited-state lifetime ($800 \mu\text{s}$). An echo efficiency of the order of 0.1% was achieved with pulse intensities 2 orders of magnitude less than those needed for a single-shot process. These results fit well an analytic solution of the Bloch equations and a three-level system relaxation model. © 2001 Optical Society of America

OCIS codes: 300.6240, 050.2770, 160.5690, 200.4740, 300.6250, 020.1670.

1. INTRODUCTION

The accumulation of a spectral grating is an efficient way to enhance the strength of stimulated-photon-echo signals.¹ This process involves the building up of a spectral grating in an inhomogeneously broadened absorbing medium by repetitive application of a pair of temporally separated programming pulses. To achieve substantial accumulation requires that the repetition period be shorter than the relaxation time of the spectral grating but longer than the coherence dephasing time. Long relaxation times can result from either a long-lived excited state (two-level systems) or a metastable bottleneck state (three-level systems). In an extreme case of persistent media, there is no upper limit on the repetition period. After the repetitive programming pulses have been applied for several relaxation times, the accumulated grating reaches a steady-state value. Optimizing the pulse intensities and material parameters for a given repetition rate produces strong echoes with programming pulses that are weak compared with those required for single-shot echo generation. Most significantly, the accumulation processes may be carried out with temporally complex pulses and therefore have applications in optical true-time delay, processing, and memory systems.²

For broadband operation, the lower input intensity requirement of accumulated gratings avoids problems with medium damage. Single-shot echo efficiency is maximized for pulse areas of $\pi/2$ on each programming pulse. For the rare-earth-doped crystal used in our experiments the intensity needed for a $\pi/2$ pulse with a 20-GHz bandwidth is of the same order as the bulk damage threshold of the laser-polished crystal. The intensity required for efficient accumulated echoes is more than 2 orders of magnitude less. In addition, achieving efficient operation with low-power laser sources is a necessary step toward developing commercial optical coherent transient (OCT) devices.

The accumulated-photon-echo technique has been used in time-domain spectroscopy of rare-earth-doped crystals as well as in demonstrations of OCT storage and processing devices.³⁻⁵ In these experiments, as in all previous

demonstrations of OCT devices, the programming and processing stages were separated in time. The processing ability lasted only for the lifetime of the spectral grating, and the dynamics of the grating while it was accumulating were not significant. Recently, the use of a continuously programmed continuous processor to achieve continuous, real-time processing capability in nonpersistent hole-burning medium was proposed.² Instead of separate programming and processing stages, the continuously programmed continuous processor has programming and data pulses applied simultaneously to the medium. The recorded pattern is accumulated and maintained by repetition of the structured programming pulses while the data stream passes through the medium continuously, generating a continuously processed output signal. Unlimited by the bottleneck lifetime, the processing ability in a nonpersistent medium can last indefinitely. Most significantly, the echo efficiency, defined as the ratio of the output signal power to the power of the input data stream, can be of the same order of magnitude for high-bandwidth accumulated OCT processors as for low-bandwidth single-shot OCT processors.² To realize practical devices based on continuous programming, appropriate nonpersistent spectral hole-burning media must be developed and their accumulation and decay mechanisms well understood.

In this paper we report what we believe to be the first experimental study of the dynamics of high-bandwidth spectral grating accumulation and decay in a nonpersistent material. In the research presented in this paper we studied the ${}^3H_6-{}^3H_4$ transition of $\text{Tm}^{3+}:\text{YAG}$ because of the following properties that make this material a promising candidate for continuous programming^{2,6,7}: (1) convenient operating wavelength at 793 nm, where commercial diode lasers as well as solid state (Ti:sapphire) continuous-wave and mode-locked pulsed lasers are available, (2) favorable temporal and spectral parameters, in particular a coherent dephasing time, T_2 , of tens of microseconds at liquid-helium temperature and an inhomogeneous spectrum of 17 GHz, which give a time-bandwidth product of the order of 10^5 at a projected data rate over 10 GHz, and (3) the presence of a metastable

state (3F_4) in the population relaxation path with an ~ 10 ms lifetime.⁷⁻⁹

This paper is organized as follows: In Section 2 we present an experiment with accumulated spectral gratings that uses picosecond programming and read pulses. In Section 3 an analytical solution to the Bloch equations, including empirical decay constants, is presented and is used to simulate the experiment. The complication of combined spectral gratings composed of programming and probe pulses is also discussed. Section 4 details the second experiment designed to eliminate the complication of combined spectral gratings. The dynamics of the desired grating, formed only by programming pulses, is observed and fitted with the theoretical model. A summary is given in Section 5.

2. EXPERIMENT

Spectral hole-burning memory and signal-processing devices in rare-earth-doped crystals have been studied primarily with acousto-optically modulated cw lasers, which limits their operational bandwidth to less than a gigahertz. Whereas practical hole-burning based devices will eventually employ compact diode and solid-state lasers, we used a picosecond Ti:sapphire mode-locked pulsed laser system with a regenerative amplifier to investigate the high-bandwidth capabilities of Tm^{3+} :YAG. An important characteristic of the laser used is its ability to de-

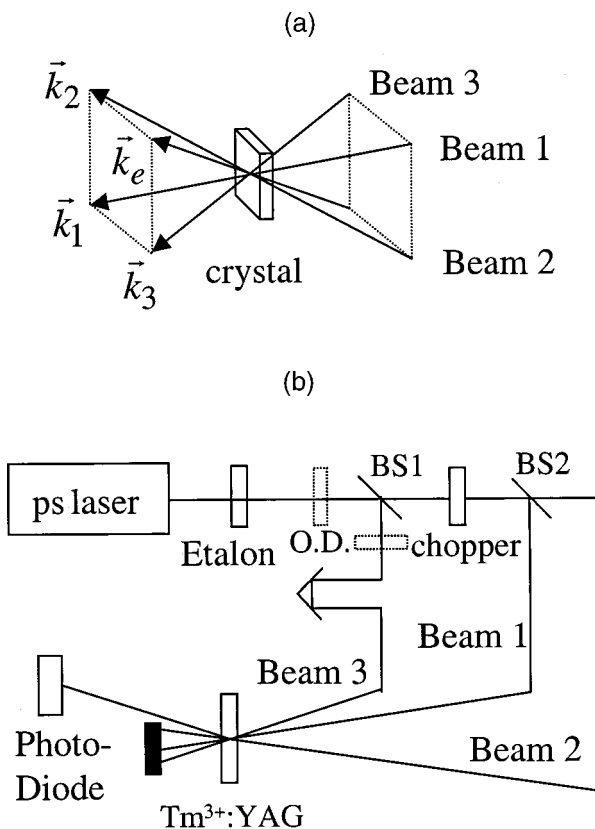


Fig. 1. (a) Box configuration. (b) Schematic of the experimental setup. In the second set of experiments the chopper was replaced by an AOM, and the O.D. was used in both locations shown. BS1 and BS2, beam splitters 1 and 2.

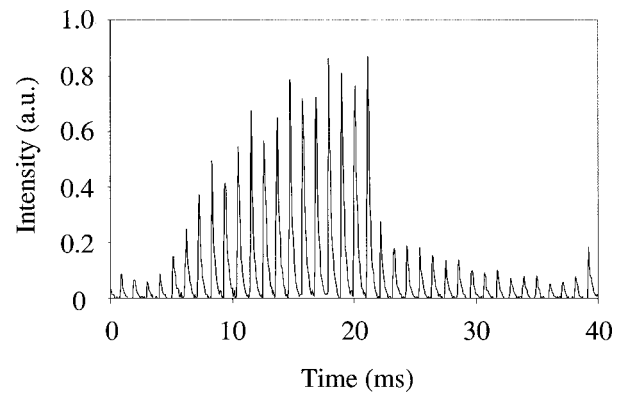


Fig. 2. Recording of echoes at a 1-kHz repetition rate with 16 laser shots of programming and probe beams unblocked followed by 16 laser shots with probe pulses only.

liver Fourier-transform-limited, 7-ps 300- μJ pulses at a repetition rate greater than 1 kHz. To avoid crystal damage, we use an external etalon to spectrally filter the laser pulse to achieve 30-ps 50- μJ laser pulses. The resultant pulse bandwidth is approximately a factor of 2 greater than the medium bandwidth (17 GHz). A schematic of the experimental setup is shown in Fig. 1. The optical pathway is split into three beams. The two programming pulses, separated by delay time τ_{21} , propagate along beams 1 and 2, respectively, and the probe pulse propagates along beam 3 with a delay τ_{32} with respect to beam 2 (see Fig. 1). The desired spectral grating formed by programming pulse pairs has a period of $1/\tau_{21}$. Laser-frequency shifts result only in shifts in the grating envelope but have no effect on the phase of the spectral grating, which is determined solely by the difference in the two optical paths. Therefore the Fourier-transform-limited pulse pairs can constructively accumulate gratings over many laser shots, provided that the laser-frequency fluctuations are less than the inhomogeneous linewidth of the medium and the path-length jitter is much less than an optical wavelength.

In our experiment we used a 5.5-mm-long Tm^{3+} :YAG crystal with a 0.1% doping concentration corresponding to an optical density of ~ 0.43 at 793 nm. The crystal was held at 4 K in a liquid-helium cryostat. The three beams were roughly equal (within a few percent) in power and were focused by a lens to cross in the crystal with a spot size ~ 0.25 mm in diameter. The wave vectors of the two programming beams, the probe beam, and the echo beams, labeled \mathbf{k}_1 , \mathbf{k}_2 , \mathbf{k}_3 , and \mathbf{k}_e , respectively, satisfy the phase-matching condition: $\mathbf{k}_e = \mathbf{k}_3 + \mathbf{k}_2 - \mathbf{k}_1$. In the continuous programming scheme the processed output is spatially isolated from the transmitted inputs by phase matching with a box geometry. The transmitted inputs were blocked after the cryostat. The output power of the echo signal was detected by a photodiode and recorded by a digital oscilloscope. The delay between the pulses on beams 1 and 2 was set to $\tau_{21} = 0.7$ ns, and that between beams 2 and 3 was $\tau_{32} = 0.2$ ns; both times were much shorter than T_2 , the homogeneous lifetime of the material. The time interval between two shots, τ_R , was

of the same order as excited-state lifetime T_1 , which is much longer than T_2 and shorter than the bottleneck-state lifetime, $T_3 \sim 10$ ms.

We studied the dynamics of the accumulated grating by inserting an optical chopper between beam splitters 1 and 2 to periodically block and unblock the programming pulses while beam 3 with the probe pulses remained unblocked. The chopper was synchronized with the laser at a subharmonic of the laser repetition frequency. A recording of echoes is shown in Fig. 2, for which the laser frequency was 1 kHz and the chopper frequency was set to (1/32) kHz, yielding 16 accumulation shots with programming pulses unblocked and 16 grating probe shots with them blocked. A neutral-density filter with an O.D. of roughly 0.5 was placed on beam 3 to prevent saturation from the probe. The output data in Fig. 2 show a pulse train at 1 kHz of stimulated photon echoes spatially isolated from the input beams and occurring 0.7 ns after the corresponding pulse on beam 3. When the programming pair is unblocked (at $t = 5$ ms), the echo intensity increases with each application of the programming pulses and tends to a steady state for large numbers of accumulation shots. After the programming beams are turned off (at $t = 22$ ms), the echo signal stimulated from the residual grating drops dramatically within 1 ms and then decays away on a time scale of 10 ms. The pulses before 5 and after 39 ms are from the preceding and the following dynamic cycles, respectively.

3. ANALYTIC MODEL

The grating dynamics depend on material parameters T_2 , T_1 , and T_3 , the absorption length, and branch ratio β (the percentage of excited-state atoms that decay to the bottleneck rather than straight to the ground state). It also depends on the timing parameters of the experiment, τ_{21} , τ_{31} , and τ_R , and on the input pulse areas. In our experiment, the absorption length in our material was 1.0, the angles between the beams were small (1/50 rad),

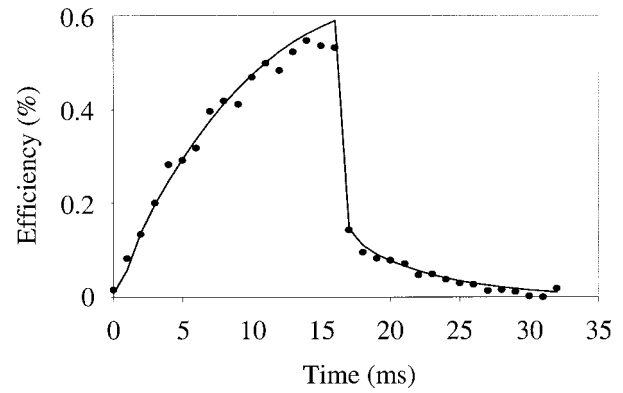


Fig. 3. Echo efficiencies measured within the programming cycle of 32 ms as for Fig. 2: experimental results (filled circles) and corresponding simulated results (curve).

mulation dynamics can be described by analytical solution of the Bloch equations with empirical decay terms. The density matrix of the system in the laser frame is

$$\rho(\Delta, t) = \begin{pmatrix} \rho_{11}(\Delta, t) \\ \rho_{12}(\Delta, t) \\ \rho_{21}(\Delta, t) \\ \rho_{22}(\Delta, t) \\ \rho_{33}(\Delta, t) \end{pmatrix}, \quad \rho(\Delta, 0) = \begin{pmatrix} 1 \\ 0 \\ 0 \\ 0 \\ 0 \end{pmatrix}, \quad (1)$$

with the constraint that $\rho_{11} + \rho_{22} + \rho_{33} = 1$. Levels 1 and 2 are the ground and excited levels of the optical transition, respectively, and level 3 is a bottleneck level between levels 1 and 2. Under the condition in which the durations τ_{21} and τ_{32} are much less than T_2 , T_1 , and T_3 , the accumulation process can be broken into two steps: a two-level system interacting with the input pulses without coherent decay and a three-level system that decays between laser shots. The interaction of a single input pulse of duration of $\tau (< T_2)$ is described by the transformation matrix¹⁰

$$A(a, \tau) = \frac{1}{2\Omega^2} \begin{bmatrix} 2\Omega^2 - aD & \Delta D - iaS & \Delta D + iaS & aD & 0 \\ \Delta D - iaS & aD + 2\Omega C + i2\Delta S & aD & -\Delta D + iaS & 0 \\ \Delta D + iaS & aD & aD + 2\Omega C - i2\Delta S & -\Delta D - iaS & 0 \\ aD & -\Delta D + iaS & -\Delta D - iaS & 2\Omega^2 - aD & 0 \\ 0 & 0 & 0 & 0 & 2\Omega^2 \end{bmatrix}, \quad (2)$$

and the spectrum of the brief pulses used was much broader than the inhomogeneous band and thus the temporal profile of the pulses could be treated as square. To derive an analytical model for the observed dynamics we made the following assumptions: an optically thin medium, a collinear beam configuration, and square temporal shape of all pulses. Under these conditions the accu-

where $C = \Omega \cos \theta$, $S = \Omega \sin \theta$, $D = a(1 - \cos \theta)$, and $\theta = \Omega \tau$. At a certain frequency Δ detuned from resonance, Rabi frequency $\Omega = \sqrt{a^2 + \Delta^2}$ is determined by on-resonance Rabi frequency a , which is proportional to the square root of the intensity of the pulse. The on-resonance pulse area is defined as $\theta = a\tau$. At time $t = 0$, the medium is in its ground state, $\rho(\Delta, 0)$. We can

also use this matrix to describe the coherent evolution of the absorbers between pulses for time intervals short compared to T_2 by setting $a = 0$ and τ equal to the time interval. For $T_2 \gg \tau, \tau_{21}, \tau_{32}$ the result of a sequence of input pulses from a single laser shot is obtained by application of Eq. (2) sequentially with the appropriate timings and Rabi frequencies. The relaxation that occurs between laser shots is described by the matrix¹¹

$$B(t) = \begin{bmatrix} 1 & 0 & 0 & 1 - \beta \exp(-t/T_3) + (\beta - 1)\exp(-t/T_1) & 1 - \exp(-t/T_3) \\ 0 & 0 & 0 & 0 & 0 \\ 0 & 0 & 0 & 0 & 0 \\ 0 & 0 & 0 & \exp(-t/T_1) & 0 \\ 0 & 0 & 0 & \beta \exp(-t/T_3) - \beta \exp(-t/T_1) & \exp(-t/T_3) \end{bmatrix}. \quad (3)$$

The coherences (ρ_{21} and ρ_{12}) are lost between two laser shots because $\tau_R \gg T_2$. The density matrix at the time of the stimulated echo generated after n programming pulse sequences (with beams 1 and 2 unblocked) and m readout sequences (with beams 1 and 2 blocked) is given by

$$\begin{aligned} \rho_{m+n}(\Delta, t_3 + \tau_{21}) &= A_{21}A_3^m B(\tau_R)^m A_3A_{32}A_2A_{21}A_1 \\ &\quad \times [B(\tau_R)A_3A_{32}A_2A_{21}A_1]^{(n-1)} \\ &\quad \times \rho(\Delta, 0), \end{aligned} \quad (4)$$

where $A_i = A(a_i, \tau_i)$, $A_{ij} = A(0, \tau_{ij})$, and t_3 is the time of the last probe pulse. The echo amplitude at time $t_3 + \tau_{21}$ after n programming shots and m probe shots is obtained by integration of $i[\rho_{21}(\Delta, t_3 + \tau_{21}) - \rho_{12}(\Delta, t_3 + \tau_{21})]g(\Delta)$ over all Δ . This method was used to simulate the grating dynamics in Fig. 2. The calculated and experimental results are plotted in Fig. 3 and are represented by a solid curve and filled circles, respectively. The fit parameters are $\theta_1 = \theta_2 = 0.08\pi$ and $\theta_3 = 0.044\pi$, and $T_3 = 13$ ms. Despite the Gaussian spatial profile of the beams, which yields a distribution of Rabi frequencies across the wave fronts, the simulation fits the experimental results well. The sudden drop after the programming beams are blocked is due to two effects. The first is the decay of the excited-state grating to the ground state. The lifetime of the excited state, T_1 , is 800 μ s, and the branching ratio, β , is 0.56, which results in a drop of 10%. The second effect is more significant because a second grating accumulates in the medium, which results in an echo at the same time and in the same direction as the expected signal. This echo results from beams 1 and 3 acting as programming beams and beam 2 acting as a probe beam. The echo is phase matched in the same direction as the echo that results from pulse 3 probing the grating of beams 1 and 2. This added contribution to the echo signal occurs only when beams 1 and 2 are unblocked because it is stimulated by beam 2. The

contributions are roughly equal in amplitude, and the signal detected is the square of the output amplitude. We see a drop of roughly a factor of 4 because of this effect after beams 1 and 2 are blocked. The decay after this sudden drop and after the excited state has decayed completely is due to the decay of the bottleneck state back to the ground state. The lifetime of the bottleneck state, T_3 , is ~ 10 ms.

4. SINGLE-GRATING DYNAMICS

The accumulation and decay of the combined gratings built by beams 1, and 2 and by beams 1 and 3 do not mimic what is expected in an OCT processor. Typically, the phase relationship between pulses 1 and 2 would be the same for all programming pulse pairs to yield coherent accumulation, whereas pulse 3 would be an uncorrelated data stream and incoherent with respect to pulses 1 and 2. To demonstrate the dynamics of the single grating under these conditions we substituted an acousto-optic modulator (AOM) in place of the chopper. The AOM has the effect of adding a random phase equally to both beams 1 and 2, as the AOM's frequency is not synchronized with the laser repetition rate. Therefore pulses 1 and 2 had a constant phase relation with respect to each other but a random phase relation with respect to pulse 3. Thus the grating that is due to beams 1 and 2 accumulated coherently, whereas the grating that is due to beams 1 and 3 accumulated incoherently. The ratio of the signals from these two gratings drops roughly with the number of laser shots. The echo signals generated by the coherent and incoherent gratings could add constructively or destructively, but on average the combined signal would be that of only the coherent grating. Thus, we can simulate the data from our AOM experiment by assuming that the grating that is due to pulses 1 and 3 is not formed. We do this by introducing into Eq. (4) a coherence loss $[B(0)]$ between pulses 2 and 3. The modified equation is

$$\begin{aligned} \rho_{m+n}(\Delta, t_3 + \tau_{21}) &= A_{21}A_3^m B(\tau_R)^m A_3B(0)A_2A_{21}A_1 \\ &\quad \times [B(\tau_R)A_3B(0)A_2A_{21}A_1]^{(n-1)} \\ &\quad \times \rho(\Delta, 0). \end{aligned} \quad (5)$$

The introduction of the AOM also allowed for longer accumulation times (no longer limited by the timing jitter of the chopper that increased with decreasing chopper frequency).

Figure 4 shows the results for 38 laser shots with all 3 beams unblocked followed by 26 laser shots with only the

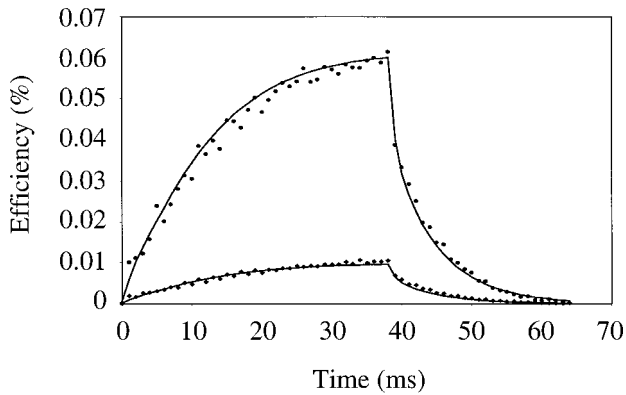


Fig. 4. Echo efficiencies at a 1-kHz repetition rate within the programming cycle of 64 ms with 38 programming and probe laser shots and 26 probe-only laser shots: experimental results for the average of 512 cycles (filled circles) and simulation (curves).

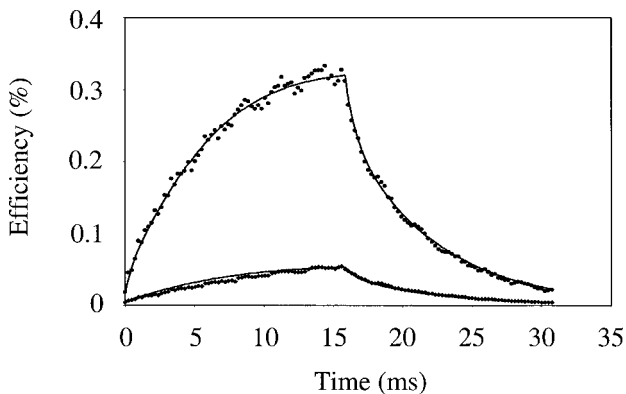


Fig. 5. Echo efficiencies at a 4-kHz repetition rate within the programming cycle of 31 ms with 66 programming and probe laser shots and 62 probe-only laser shots: experimental results of the average of 512 cycles (filled circles) and simulation (curves).

probe beam unblocked. The data represent the average of 512 buildup and decay cycles. We no longer see the dramatic drop when pulses 1 and 2 are blocked. The fluctuations of the echo signal during accumulation are likely the result of the incoherent buildup of the grating owing to pulses 1 and 3. The maximum echo efficiency is $\sim 0.06\%$. The fit parameters for the upper curve are $\theta_1 = \theta_2 = 0.039\pi$ and $\theta_3 = 0.024\pi$, and $T_3 = 13$ ms. To test the validity of our model we moved the neutral-density filter in front of beam splitter 1, which attenuated all three beams, yielding the results of the lower curve. The fit parameter for the lower curve is $\theta_1 = \theta_2 = \theta_3 = 0.024\pi$, and $T_3 = 13$ ms.

For the data in Figs. 3 and 4 the laser repetition period of 1 ms was greater than the excited-state lifetime of 0.8 ms. To investigate the accumulation dynamics when the repetition period is shorter than the excited state lifetime, we increased the repetition rate to 4 kHz (the laser's maximum repetition rate). The AOM was set to allow for 66 programming and probe laser shots and 62 probe-only laser shots. Figure 5 shows the results for full (O.D. in beam 3 only, upper trace) and attenuated (O.D. in all beams, lower trace) programmings, with an average of 512 buildup and decay cycles. The fit parameters are the same as for Fig. 4, as expected, because the laser pulse energies were roughly the same in both cases. The echo

efficiency for full programming power (upper curve) was $\sim 0.3\%$, close to the value expected.

According to the calculation in Ref. 2, the photon echo signal from an optimized accumulated grating can reach 1/8 of that caused by $\pi/2$ single shots and one can always optimize the accumulation at a given τ_R by varying the programming pulse area to an optimal value θ_{op} . In general, a long τ_R requires a large θ_{op} . In our experiment, τ_R is restricted to be longer than 250 μ s by the maximum repetition rate (4 kHz) of the regenerative amplifier in the laser system. Our simulation resulted in $\theta_{op} = 0.15\pi$ for 4 kHz and $\theta_{op} = 0.3\pi$ for 1 kHz. Although the pulse areas in the experiments were much lower than the optimal values, a further increase was difficult because of the risk of high-peak-power damage in the crystal. When the pulse area is less than the optimal value, a decreased repetition period is a way to increase the echo efficiency. The experimental results from 1 to 4 kHz in Figs. 4 and 5, respectively, show the trend. Theoretically, the smallest τ_R can be 32 μ s ($2T_2$) for $\text{Tm}^{3+}:\text{YAG}$, and the pulse area is optimized at $\theta_{op} = 0.05\pi$. Unfortunately, no broadband laser source is available to meet the requirements. One may consider using the pulses directly from the oscillator at 80 MHz if T_2 can be shortened to nanoseconds (by power-induced spectral diffusion or an increase in temperature, for example). However, comparing the pulse energy and length, 10 μ J/30 ps (1 nJ/100 fs) with (without) a regenerative amplifier, we estimate the echo efficiency to be 10^4 times less in the case without the regenerative amplifier. So the echo efficiency, $\sim 0.3\%$ in Fig. 5, is the maximum value that we can reach experimentally under current conditions.

5. SUMMARY

In summary, the dynamics of high-bandwidth accumulated spectral gratings has been experimentally observed in $\text{Tm}^{3+}:\text{YAG}$ by means of stimulated photon echoes. The accumulation dynamics were studied under several conditions, and the results matched the analytic model well in all cases. An echo intensity efficiency of the order of 0.1% has been observed. These results are an important step in the demonstration of a continuously programmed true-time-delay processor that works on broadband signals.

ACKNOWLEDGMENTS

We gratefully acknowledge the support of this research by the U.S. Office of Naval Research and the University of Colorado under the Multidisciplinary University Research Initiative Program (grant N00014-97-1-1006). We thank Randy Equall of Scientific Material, Inc., for discussions of laser damage in $\text{Tm}:\text{YAG}$ and for fabrication of the sample used.

REFERENCES

1. W. H. Hesselink and D. A. Wiersma, "Picosecond photon echoes stimulated from an accumulated grating," *Phys. Rev. Lett.* **43**, 1991-1994 (1979).
2. K. D. Merkel and W. R. Babbitt, "Optical coherent transient

- continuously programmed continuous processor,” *Opt. Lett.* **24**, 172–174 (1999).
3. M. Mitsunaga and N. Uesugi, “248-Bit optical data storage in $\text{Eu}^{3+}:\text{YAlO}_3$ by accumulated photon echoes,” *Opt. Lett.* **15**, 195–197 (1990).
 4. M. Mitsunaga, R. Yano, and N. Uesugi, “Time- and frequency-domain hybrid optical memory: 1.6-kbit data storage in $\text{Eu}^{3+}:\text{Y}_2\text{SiO}_5$,” *Opt. Lett.* **16**, 1890–1892 (1991).
 5. V. A. Zuikov, D. F. Gainulin, V. V. Samartsev, M. F. Stel'makh, M. A. Yufin, and M. A. Yakshin, “Accumulated long-lived optical echo and optical memory,” *Sov. J. Quantum Electron.* **21**, 477–478 (1991).
 6. R. M. Macfarlane, “Spectral hole burning in the trivalent thulium ion,” *Opt. Lett.* **18**, 829–831 (1993).
 7. R. M. Macfarlane, “Photon-echo measurement on the trivalent thulium ion,” *Opt. Lett.* **18**, 1958–1960 (1993).
 8. J. A. Caird, L. G. Deshazer, and J. Nella, “Characteristics of room-temperature 2.3- μm laser emission from Tm^{3+} in YAG and YAlO_3 ,” *IEEE J. Quantum Electron.* **QE-11**, 874–881 (1975).
 9. N. M. Strickland, P. B. Sellin, Y. Sun, J. L. Carlsten, and R. L. Cone, “Laser frequency stabilization using regenerative spectral hole burning,” *Phys. Rev. B* **62**, 1473–1475 (2000).
 10. L. Allen and J. H. Eberley, *Optical Resonance and Two-Level Atoms* (Dover, New York, 1987), p. 58.
 11. W. H. Hesselink and D. A. Wiersma, “Photon echoes stimulated from an accumulated grating: theory of generation and detection,” *J. Chem. Phys.* **75**, 4192–4197 (1981).